Luminescent-wavelength tailoring silicon-rich silicon nitride LED

Cheng-Tao Lin (林政道), Cheewee Liu (劉致爲), and Gong-Ru Lin (林恭如)*

Graduate Institute of Photonics and Optoelectronics, Department of Electrical Engineering,
National Taiwan University, No. 1 Roosevelt Road Sec. 4, Taipei 106
**E-mail: grlin@ntu.edu.tw*

Received September 17, 2008

Wavelength tunable photoluminescence (PL) of Si-rich silicon nitride (SRSN) film with buried Si nanocrystals (Si-ncs) grown by plasma enhanced chemical vapor deposition (PECVD) under SiH_4 and NH_3 environment is investigated. Intense broadband visible emissions tunable from blue to red can be obtained from the as-deposited SiN_x thin films with increasing NH_3 flow rate from 150 to 250 sccm and detuning the SiH_4/NH_3 flow ratio during deposition. To date, the normalized PL wavelength of SiN_x films after annealing could be detuned over the range of 385−675 nm by decreasing the NH_3 flow rate, corresponding to an enlargement on Si-nc size from 1.5−2 to 4−5 nm. The PL linewidth is decreased with increasing ammonia flow rate due to the improved uniformity of Si-ncs under high NH_3 flow rate condition. In addition, the PL intensity is monotonically increasing with the blue shift of PL wavelength due to the increasing density of small-size Si-ncs. The ITO/SiN_x/p-Si/Al diode reveals highly resistive property with the turn-on voltage and power-voltage slope of only 20 V and 0.18 nW/V, respectively. The turn-on voltage can further reduce from 20 to 3.8 V by improving the carrier injection efficiency with p-type Si nano-rods.

OCIS codes: 160.4670, 230.3670, 230.5590.
doi: 10.3788/COL20090704.0277.

The research on nanocrystallite Si based light-emitting materials has attracted much attention because of their manufacturing compatibility and potential applications in realization of all-Si-based photonic integrated circuits. Although bulk Si has an indirect band gap, stable efficient light emission can be achieved in Si nanostructures at room temperature where the selection rule is broken and the quantum confinement effect predominates the improved luminescent mechanism. The first discovery of luminescence from Si nanostructure was demonstrated using a Si quantum wire array formed in porous Si material by Canham in 1990[1]. Then the photoluminescence (PL) of Si nanocrystals (Si-ncs) buried in Si dioxide was studied by Littau *et al.* in 1993[2]. The Si nano-particle colloid is made by homogeneous gas-phase nucleation following pyrolysis of the dilute disilane in He gas. Later on, versatile technologies have been proposed for synthesizing buried Si-ncs in either plasma enhanced chemical vapor deposition (PECVD) grown Si-rich oxide (SiO_x) or nitride (SiN_x) film after high-temperature annealing[3,4]. The metal-oxide-semiconductor (MOS) diode made of aforementioned oxide or nitride film is able to emit light under current injection, however, the electric field needed for electroluminescence (EL) in SiO_x is larger than 6 MV/cm for electron injection and more than 10 MV/cm for hole injection from Si into SiO_2[5,6]. Such an electric field is approaching the soft-breakdown region of a SiO_2 film. This constrain on biased voltage can somewhat be released by employing the SiN_x material as the host matrix for Si-ncs. The SiN_x exhibits several potential advantages over SiO_x, such as the low band gap energy of 4.6 eV for Si_3N_4[7], and the relatively small barriers of 2.0 and 1.5 eV for electrons and holes, respectively, at the Si-Si_3N_4 interface. Hence an electric field of 2−4 MV/cm is already sufficient for double (electron and hole) injection into Si_3N_4[8], which is much lower than the breakdown field (~9 MV/cm) of Si_3N_4[9]. The first study on Si-ncs within SiN_x films deposited by low pressure chemical vapor deposition (LPCVD) was proposed by Volodin *et al.*[10]. In addition to the benefit on electrical property, it was also reported that the Si-ncs in SiN_x exhibited superior luminescent capability over Si-ncs in SiO_x with similar synthesized condition[11]. Afterwards, the PL wavelength detuned by controlling the size of Si-ncs ranging from 1.5 to 5 nm has been demonstrated[12,13]. Although there were many kinds of reactant gas recipes used to form Si-rich silicon nitride (SRSN) films, such as SiH_4/N_2, SiH_4/NH_3, and SiH_2Cl_2/NH_3, the significant enhancement on Si-nc related PL intensity is observed using SiH_4/NH_3. This is attributed to hydrogen passivation of non-radiative defects under the hydrogen-rich growth condition as compared to the conventional SiH_4/N_2 recipe[14]. However, few literatures related to the EL emission of SRSN films with buried Si-ncs were demonstrated. In this letter, we successfully deposit the PL-wavelength tunable SRSN films by detuning the ammonia flow rate during PECVD growth. Current-voltage and power-voltage characteristics of the MOS light-emitting diodes (LEDs) made on the annealed SRSN film containing Si-ncs with significant crystalline lattice shown by transmission electron microscopy (TEM) photograph are discussed.

The Si-rich SiN_x films were deposited on (100)-oriented Si substrate with resistivity of 1−5 Ω·cm using a conventional PECVD system. By using NH_3 and SiH_4 mixed gas recipe, the samples were prepared at a chamber with the pressure of 67 Pa, a forward radio frequency (RF) power of 200 W, and a substrate temperature of 250 °C.

1671-7694/2009/040277-03

The flow rate of SiH_4 was kept at a constant of 250 sccm and the various conditions on the flow rate NH_3 ranging from 150 to 250 sccm were selected to grow the SiN_x film. Although there was already a visible but weak PL emission revealed on the as-deposited samples, the optimum annealing temperature and duration were determined to induce more precipitation of Si-ncs in the SiN_x for higher PL intensity. During the annealing process in a quartz furnace with N_2 flowing environment, the temperature and time ranged from 900 to 1000 °C and from 15 to 90 min, respectively. The thickness of the annealed Si-rich SiN_x sample containing Si-ncs was determined by α-step measurement after etching. After annealing, the room-temperature continuous-wave (CW) PL test was performed by using a He-Cd laser based pumping beam at the wavelength of 325 nm and average power of 50 W. The PL from 350 to 900 nm was resolved by a monochromator using a 3000-g/mm grating (CVI, DK240) and a photomultiplier tube (Hamamatsu, R928). The working distance between the focusing lens and samples was fine tuned to maximize the PL intensity. A TEM was used to characterize the orientation, lattice constant, size, and density of the precipitated Si-ncs in annealed SiN_x. At last, we fabricated the ITO/SiN_x/p-Si/Al diodes by Al evaporation and indium tin oxide (ITO) sputtering instruments, in order to measure the electrical and EL properties of the SiN_x based MOS LEDs.

As a result, the wavelength tunable PL spectra of the post-annealed SRSN films with buried Si-ncs grown by PECVD under detuned NH_3 flow rate were demonstrated. We have observed the intense broadband visible emissions from the annealed SiN_x thin films, which are tunable from blue to red with the NH_3 flow rate increasing from 150 to 250 sccm. The SiH_4/NH_3 flow ratio is concurrently decreasing at a constant SiH_4 flow rate during the PECVD growth. To date, the central PL wavelength of the annealed SiN_x films could be widely tuned over the range of 385−675 nm, as shown in Fig. 1. This result related to the blue shift of PL is mainly due to the reduction of the size of Si-ncs when increasing the ammonia flow rate. By gradually increasing the NH_3 flow rate, the N/Si composition ratio of the as-grown SiN_x film is enlarged and the volume density of the excess Si atoms embedded in the Si_3N_4 matrix is decreased. In this case, the size of Si-ncs precipitated after furnace annealing is approximately reduced by a factor of the N/Si ratio. Therefore, the PL wavelength is easily detuned by changing the N/Si composition ratio of SiN_x.

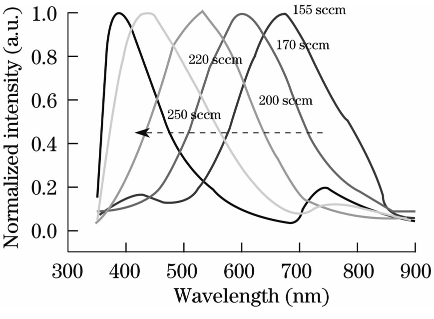

Fig. 1. Tunable PL of annealed Si-rich SiN_x films grown at different NH_3 flow rates.

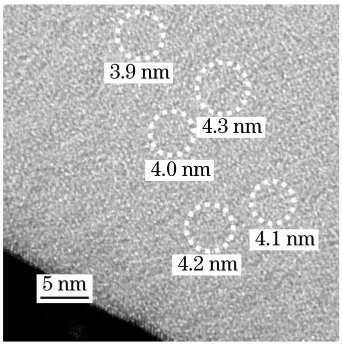

Fig. 2. Cross-section view TEM photograph of Si-ncs in Si-rich SiN_x film grown at NH_3 flow rate of 150 sccm.

The Si-ncs precipitated in the Si-rich film grown with NH_3 flow rate of 150 sccm could be observed by TEM, as shown in Fig. 2. The formation of Si-ncs with distinct lattice plane and size of 4±1 nm is obtained in this condition. In addition, the full-width at half-maximum (FWHM) of PL spectrum is significantly decreased as the ammonia flow rate increases, because the uniformity of Si-ncs size with higher NH_3 flow rate is better than that with lower NH_3 flow rate. For example, the spectral width is greatly reduced from 220 to 100 nm as the NH_3 flow rate increases from 150 to 250 sccm. Due to the reduced volume density, the size distribution of the precipitated Si-ncs is strictly limited within a small range. On the contrary, the PL intensity is monotonically increasing with the blue shift of PL wavelength at the NH_3 flow rate below 200 sccm, which is due to the increasing density of small-size Si-ncs at a slightly decreased N/Si composition ratio. At NH_3 flow rate beyond 200 sccm, the N/Si composition is rapidly enlarged, contributing to a distinct reduction of excessive Si atoms in the matrix, such that the PL intensity normalized to film thickness turns to decrease oppositely.

For El analysis, the ITO/SiN_x/p-Si/Al diode based MOS LED made of the annealed SiN_x film reveals highly resistive property with the turn-on voltage and power-voltage (P-V) slope of only 20 V and 0.18 nW/V, respectively, as shown in Figs.3 and 4. Such a turn-on voltage of SRSN diode was extremely lower than that of Si-rich Si dioxide (SRSO). This is because of the lower barrier height at the metal and Si_3N_4 interface. Nonetheless, a maximum EL power of only 5 nW was revealed on the MOS LED sample with SiN_x film thickness of 80 nm at a turn-on voltage of 15 V. By improving the carrier injection efficiency with the p-type Si nano-rod array of optimized height and density on Si substrate, we observed the turn-on voltage reducing from 20 to 3.8 V, however, the breakdown voltage of SRSN films were concurrently decreased. On the other hand, the maximum EL power reaches 40 nW under the current limitation of voltage source. The EL power is also saturated as the current approaches the upper limit of diagnostic system, in which the slope of this power-voltage curve is increasing up to 2 nW/V. The aforementioned results present an alternative carrier transport directly from the tip of Si nano-rod to the Si-nc and to the top ITO contact, however, most of the carriers pass through the SRSN film without dropping into the Si-nc. Even though the metal-Si_3N_4 interfacial barrier

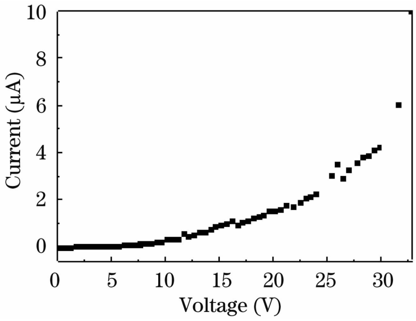

Fig. 3. Current-voltage characteristic of SRSN based MOS LED.

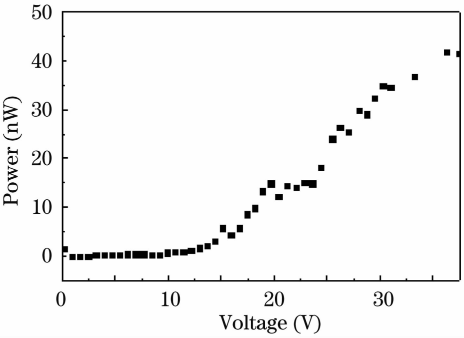

Fig. 4. Power-voltage characteristic of SRSN based MOS LED.

is greatly reduced to facilitate the carrier tunneling, the catching and recombination rates of carriers in the Si-ncs are relatively low. This indicates that the enhancement on EL via the tunneling mechanism induced carrier injection in the MOS LED is not efficient, which has to be re-considered for optimizing the EL power and efficiency of the SiN_x based MOS LED.

In conclusion, the wavelength tunable PL of SRSN film with buried Si-ncs grown by PECVD under $\mathrm{SiH_4}$ and $\mathrm{NH_3}$ environment is investigated. The Si-ncs in SRSN with diameter of 4−5 nm and distinct lattice plane grown at $\mathrm{NH_3}$ flow rate of 150 sccm could be observed by TEM. Intense broadband visible emissions tunable from blue to red can be obtained from the as-deposited SiN_x thin films with increasing $\mathrm{NH_3}$ flow rate from 150 to 250 sccm and detuning the $\mathrm{SiH_4/NH_3}$ flow ratio during deposition. The normalized PL wavelength of SiN_x films after annealing could be detuned over the range of 385−675 nm. This result related to the blue shift of PL is due to the reduction of the size of Si-ncs when ammonia flow rate increases. In addition, the FWHM of PL decreases as ammonia flow rate increasing, because the uniformity of Si-ncs with high $\mathrm{NH_3}$ flow rate is better than that with low $\mathrm{NH_3}$ flow rate. Based on this result, we could deposit SiN_x films with various colorful emission by detuning ammonia flow rate. In particular, the PL intensity is monotonically increasing with the blue shift of PL wavelength due to the increasing density of small-size Si-ncs. The ITO/SiN_x /p-Si/Al diode made of the SiN_x reveals highly resistive property with the turn-on voltage and power-voltage slope of only 20 V and 0.18 nW/V, respectively. By improving the carrier injection efficiency with a p-type Si nano-rod array substrate, we observed the turn-on voltage reducing from 20 to 3.8 V, however, the breakdown voltage of SRSN films were concurrently decreased with the increasing densities and height of Si rods. These results present an alternative carrier transport directly from Si nano-rod to top ITO electrode without recombination in the Si-ncs, which indicates that the enhancement on carrier injection via the tunneling mechanism has to be re-considered.

This work was partially supported by the National Science Council under Grants No. NSC97-2221-E-002-055 and NSC97-ET-7-002-007-ET.

References

1. L. T. Canham, Appl. Phys. Lett. **57,** 1046 (1990).
2. K. A. Littau, P. J. Szajowski, A. J. Muller, A. R. Kortan, and L. E. Brus, J. Phys. Chem. **97,** 1224 (1993).
3. A. Pérez-Rodríguez, O. González-Varona, B. Garrido, P. Pellegrino, J. R. Morante, C. Bonafos, M. Carrada, and A. Claverie, J. Appl. Phys. **94,** 254 (2003).
4. D. Pacifici, E. C. Moreira, G. Franzò, V. Martorino, F. Priolo, and F. Iacona, Phys. Rev. B **65,** 144109 (2002).
5. D. J. DiMaria, J. R. Kirtley, E. J. Pakulis, D. W. Dong, T. S. Kuan, F. L. Pesavento, T. N. Theis, J. A. Cutro, and S. D. Brorson, J. Appl. Phys. **56,** 401 (1984).
6. V. A. Gritsenko, *Structure and Electronic Properties of Amorphous Insulators in Silicon MIS Structures* (Science, Novosibirsk, 1993).
7. V. A. Gritsenko, in *Silicon Nitride in Electronics* V. I. Belyi, (ed.) (Elsevier, New York, 1988).
8. V. A. Gritsenko and E. E. Meerson, Sov. Microelectron. **17,** 249 (1988).
9. V. A. Gritsenko and E. E. Meerson, Phys. Stat. Sol. (a) **62,** K131 (1980).
10. V. A. Volodin, M. D. Efremov, and V. A. Gritsenko, Solid State Phenomena **57−58,** 501 (1997).
11. Y. Q. Wang, Y. G. Wang, L. Cao, and Z. X. Cao, Appl. Phys. Lett. **83,** 3474 (2003).
12. H.-S. Kwack, Y. Sun, Y.-H. Cho, N.-M. park, and S.-J. park, Appl. Phys. Lett. **83,** 2901 (2003).
13. Z. T. Kang, B. K. Wagner, J. Parrish, D. Schiff, and C. J. Summers, Nanotechnol. **18,** 415709 (2007).
14. C.-H. Cho, B.-H. Kim, T.-W. Kim, S.-J. Park, N.-M. Park, and G.-Y. Sung, Appl. Phys. Lett. **86,** 143107 (2005).